International Journal of Pharmacy and Pharmaceutical Research (IJPPR)
Volume 32, Issue 4, April 2026 ijppr.humanjournals.com ISSN: 2349-7203

Formulation and Evaluation of Hydrogel Containing Morin Bioactive Molecule for Psoriasis

Khushboo[*1], Ms. Astha Tiwari[2], Ms. Swarnim Srivastav[2]

[1]M.Pharm Research Scholar, [2]Associate Professor, Associate Professor, Aryakul College Of Pharmacy & Research, Lucknow, U.P. India.

Received: 23 February 2026 Revised: 07 March 2026 Accepted: 25 March 2026

ABSTRACT

Psoriasis is a chronic inflammatory skin disorder characterized by keratinocyte hyperproliferation, erythematous plaques, and scaling, which significantly impacts patient quality of life. The present study aimed to develop and evaluate morin-mediated silver/silver chloride (Ag/AgCl) nanoparticle-loaded hydrogels for potential topical application in psoriasis management. Morin, a naturally occurring flavonoid with anti-inflammatory, antioxidant, and immunomodulatory properties, was utilized as a reducing and stabilizing agent for the green synthesis of Ag/AgCl nanoparticles. The synthesized nanoparticles were characterized using UV–Vis spectroscopy, Fourier Transform Infrared (FTIR) spectroscopy, and X-ray diffraction (XRD), confirming their formation, crystalline nature, and functional group stabilization. Hydrogels incorporating morin nanoparticles were prepared using methylcellulose, carboxymethylcellulose, and sodium alginate and evaluated for physicochemical properties including pH, viscosity, spreadability, extrudability, and stability. In-vitro drug release studies demonstrated sustained and controlled release, with formulations MFG2 and MFG5 exhibiting optimal release profiles. Ex vivo permeation studies confirmed effective skin penetration and retention of morin. Furthermore, antimicrobial testing revealed broad-spectrum activity against Gram-positive and Gram-negative bacteria as well as Candida albicans, with formulation-dependent efficacy. Overall, morin-mediated Ag/AgCl nanoparticle hydrogels displayed favorable physicochemical characteristics, controlled drug release, and antimicrobial potential, highlighting their promise as safe, effective, and patient-friendly topical therapeutics for psoriasis and related skin infections.

Keywords: Psoriasis, Morin, Silver nanoparticles, Hydrogel, Green synthesis, Controlled drug release, Antimicrobial activity, Topical therapy

INTRODUCTION

Psoriasis is a chronic, immune-mediated inflammatory skin disorder characterized by hyperproliferation of keratinocytes, erythematous plaques, and scaling. [1, 2] It affects approximately 2–3% of the global population and significantly impacts the quality of life due to its recurrent and persistent nature. [3] Conventional therapies, including corticosteroids, immunosuppressants, and systemic agents, often present limitations such as adverse effects, low patient compliance, and lack of targeted delivery. This has driven the search for safer and more effective alternatives derived from natural bioactive compounds. [4]

Morin, a naturally occurring flavonoid found in fruits and medicinal plants, exhibits potent anti-inflammatory, antioxidant, and immunomodulatory properties, making it a promising candidate for psoriasis management. Hydrogels, as versatile drug delivery systems, provide controlled release, high water content, and enhanced skin penetration, which can improve therapeutic efficacy and patient compliance. [5, 6] The present study focuses on the formulation of a hydrogel containing morin as the bioactive molecule and its evaluation for potential anti-psoriatic activity, aiming to develop an effective, safe, and patient-friendly topical therapy.

MATERIALS AND MEHODS

The materials used in this study were procured from various suppliers. Morin was obtained from Yarrow Chem Pvt. Ltd., Mumbai. HPMC K100M and triethanolamine were procured from Loba Chem. Pvt. Ltd., Mumbai, while Gaur Gum was sourced from Anmol Chemicals, Mumbai. Carbopol 934, methanol, ethanol, chloroform, and buffer solution were purchased from E. Merck (India) Ltd., Mumbai. Sodium hydroxide was obtained from Loba Chem. Pvt. Ltd., Mumbai. Sulfuric acid, hydrochloric acid, and propylene glycol were procured from Bodal Chemicals Limited, Vadodara. Distilled water was collected from the college campus.

Biosynthesis Of Ag/AgCl NPs: The morin compound was utilized as a reducing and stabilizing agent for the green synthesis of silver nanoparticles (AgNPs). Analytical grade silver nitrate ($AgNO_3$) (A.R., 99.2%, molecular weight 169.87 g/mol), procured from Merck, South Africa, was used as the silver precursor. A 0.1 mM aqueous solution of silver nitrate was prepared by dissolving the appropriate amount in 1 liter of distilled water. Subsequently, 50 mL of the morin was added dropwise into 450 mL of this $AgNO_3$ solution under continuous stirring at ambient room temperature. The reaction was conducted in a dark chamber to prevent any photo-reduction of silver nitrate that could interfere with nanoparticle formation. The bio-reduction of silver ions (Ag^+) to elemental silver (Ag^0) was visually confirmed by the distinct color change of the solution from colorless to dark brown, indicative of the formation of silver/silver chloride nanoparticles (Ag/AgCl NPs). To separate the synthesized nanoparticles, the reaction mixture was centrifuged at 15,000 rpm at 15°C for 20 minutes. A 2 mL aliquot of the supernatant was collected for UV-Visible spectroscopic analysis to monitor nanoparticle formation. The resulting pellet was washed three times with distilled water to remove residual impurities and unreacted biomolecules. The purified nanoparticles were then oven-dried overnight at 80°C for further characterization and applications. [7, 8]

The formation, surface chemistry, and crystalline nature of the synthesized silver nanoparticles (AgNPs) were characterized using UV-Visible spectroscopy, and Fourier Transform Infrared (FT-IR) spectroscopy. UV-Visible spectroscopy was performed with a PerkinElmer spectrophotometer, scanning wavelengths from 300 to 600 nm at 1 nm resolution, using a 2 mL quartz cuvette with a 1 cm path length, to confirm nanoparticle formation and optical properties. FT-IR analysis was carried out on a Shimadzu FTIR spectrometer in the range of 4000–400 cm^{-1} at 4 cm^{-1} resolution to identify functional groups on the nanoparticle surface derived from morin. Dried AgNPs were dispersed in potassium bromide (KBr) and compressed into transparent discs, with KBr as the reference standard. XRD analysis using an X'Pert Panalytical diffractometer at 40 kV and 30 mA with Cu Kα radiation was employed to determine the crystalline structure and phase of the nanoparticles, where dried samples were scanned to obtain characteristic diffraction patterns, confirming the formation of crystalline AgNPs. [9, 10]

Formulation of the Hydrogel: Hydrogel formulations based on methylcellulose (MC) and carboxymethylcellulose (CMC) were prepared via thermal dispersion of the gelling agent in a blend of distilled water and glycerol, heated to 80 °C for MC-based systems and 50 °C for CMC-based ones. Subsequently, under room temperature conditions, the polymers were gradually incorporated into the solution and stirred at 300 rpm until uniform mixtures were obtained. In contrast, the procedure for preparing formulations containing sodium alginate (SA) involved dissolving the polymer in a water-glycerol mixture along with 200 µL of a 0.5% calcium chloride solution (used as a crosslinking agent) at ambient temperature. Morin, initially solubilized in dimethyl sulfoxide (DMSO), was subsequently introduced into the pre-formed formulations. The active compound solution was blended with the hydrogel matrix by mechanical agitation for 15 minutes. The resulting hydrogels were transferred into polyethylene containers and stored under refrigeration for further analysis. The specific compositions of the hydrogels are detailed in Table 1. [11, 12]

Table 1. The composition of hydrogels with Morin NPs

Ingredients	MGF1	MGF2	MGF3	MGF4	MGF5	MGF6
	Content (g)					
Morin NPs	0.4	0.4	0.4	0.7	0.7	0.7
Sodium alginate	4.0			4.0		
Methylcellulose	-	-	4.0	-	-	4.0
Sodium carboxymethyl cellulose	-	4.0	-	-	4.0	-
Glycol 86%	10	10	10	10	10	10
Dimethyl sulfoxide	2	2	2	2	2	2
Purified water		up to 100	up to 100	up to 100	up to 100	up to 100

Evaluation of Hydrogel Formulations: The developed morin-based hydrogel formulations were systematically evaluated for their physical, chemical, and mechanical properties. Visual and sensory inspection assessed parameters including color, appearance, homogeneity, texture, tackiness, oiliness, and adhesiveness. The pH of each formulation was measured in triplicate using a calibrated pH meter, and spreadability was evaluated by placing a fixed volume of hydrogel between glass plates under increasing weights, with the spread radius used to calculate surface area. Rheological properties, including flow behavior, viscosity, and thixotropy, were analyzed using a rotational rheometer at controlled shear rates and skin-simulating temperatures (32 ± 0.5 °C), providing insights into the hydrogel's mechanical performance and application characteristics. [13, 14]

Ex vivo skin permeation studies were conducted using Franz diffusion cells with porcine skin to assess morin penetration and retention. Hydrogel samples were applied to the stratum corneum side, and the acceptor solution was sampled at predetermined intervals over 24 hours for UV-Vis analysis. Residual drug in the skin was quantified after extraction, ensuring accurate determination of API retention. Stability studies were performed by storing the formulations at 2–8 °C for 28 days, with subsequent

evaluation of visual appearance, pH, spreadability, texture, viscosity, and API content to ensure both chemical and physical stability, confirming the hydrogel's suitability for topical application. [15, 16]

Antimicrobial Potential: The antimicrobial potential of the morin-based hydrogel formulations was evaluated against selected bacterial and fungal strains, including Staphylococcus epidermidis (clinical isolate), Staphylococcus aureus (ATCC 25923), Escherichia coli (ATCC 25922), Pseudomonas aeruginosa (ATCC 4853), and Candida albicans (clinical isolate). Mueller-Hinton broth (single and double strength) was prepared by dissolving 2.1 g or 4.2 g of the broth powder in 100 mL sterile water, followed by autoclaving at 121 °C for 30 minutes. Pure isolates were sub-cultured in the sterilized broth at 37 °C for 24 hours and streaked onto agar plates to obtain distinct colonies, ensuring the use of well-characterized microbial cultures for testing. [17]

The minimum inhibitory concentration (MIC) of the hydrogel formulations was determined using the microbroth dilution method in microtiter plates. Serial dilutions of the hydrogels were prepared in Mueller-Hinton broth, inoculated with standardized microbial suspensions (adjusted to 0.5 McFarland standard), and incubated at 37 °C for 24 hours. The MIC was defined as the lowest hydrogel concentration that completely inhibited visible microbial growth, providing a quantitative measure of antimicrobial efficacy. This approach enabled the evaluation of the hydrogel's effectiveness against both gram-positive, gram-negative bacteria, and fungi. [18, 19]

RESULTS AND DISCUSSION

UV-Vis Spectroscopy Analysis: Ag/AgCl NPs synthesis via biological means morin compound was carried out in this study. Due to its high conductivity and catalytic properties, as well as its chemical stability, silver nitrate was used as a suitable precursor. The gradual addition of the morin a (light brown colour) to silver nitrate solution resulted into the instant formation of a dark brown coloration, which could be ascribed to the completion of the reaction. For biological synthesis of nanoparticles to have added advantage over chemical methods, the time for synthesis is also a critical factor to be considered. Subsequently, UV–Vis spectroscopy was used to confirm the formation of the Ag/AgCl NPs, indicated by the appearance of the dark-brown colloidal solution, as a result of excitation of surface plasmon resonance (SPR) between 290–360 nm (Figure 1).

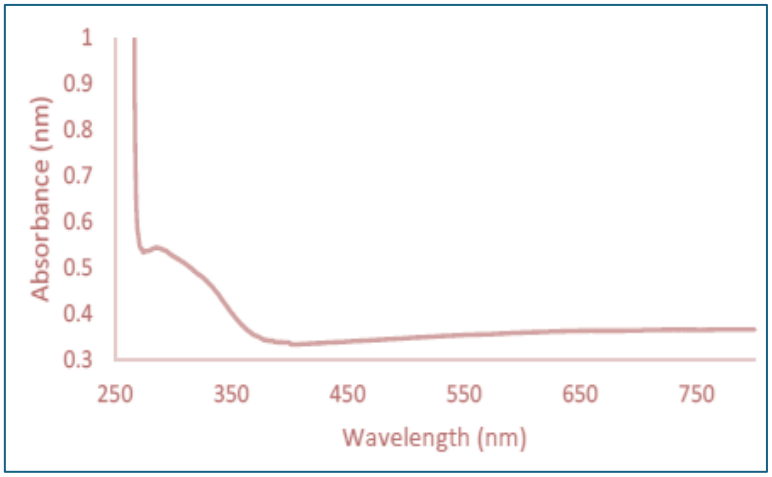

Figure 1: U.V. Spectra of silver nanoparticle

Our findings corroborate with the absorbance value of biosynthesized silver nanoparticles reported from previous studies, and contrary to our present study, some biogenic AgNPs synthesized from morin had SPR between 400 and 500 nm. The type of biogenic nanoparticles formed depends on the phytochemical compounds in the morin. The observed results show that the synthesis of Ag/AgCl NPs through the green approach in this study proved to be ancient with respect to reaction time, as well as having no requirement for the use of toxic chemical reducing or stabilizing agents. Therefore, making it an economical, sustainable, reliable, and an alternative process to chemical or physical methods for the synthesis of silver nanoparticles.

FTIR Analysis: The FTIR spectrum recorded in the range of 4000–500 cm^{-1} shows several characteristic absorption bands that indicate the presence of multiple functional groups. A broad absorption band observed around 3368 cm^{-1} is attributed to O–H stretching vibrations, suggesting the presence of hydroxyl groups, possibly involved in hydrogen bonding.

International Journal of Pharmacy and Pharmaceutical Research (IJPPR)
Volume 32, Issue 4, April 2026 ijppr.humanjournals.com ISSN: 2349-7203

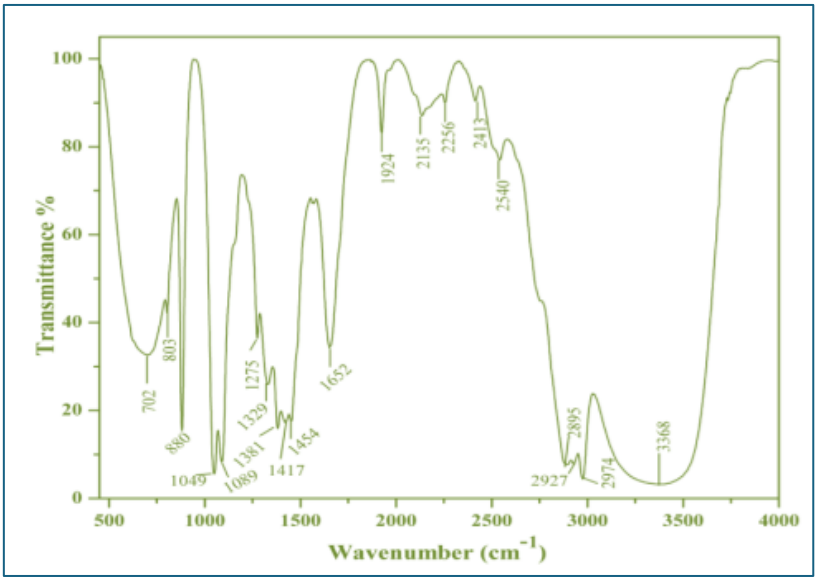

Figure 2. Transform infrared spectroscopy (FTIR) spectra of the morin AgNPs

The peaks at 2927 cm^{-1} and 2855 cm^{-1} correspond to aliphatic C–H stretching vibrations of $–CH_2$ and $–CH_3$ groups. Weak bands in the region of 2540–2312 cm^{-1} may arise from overtone or combination bands or weak triple-bond stretching vibrations. The absorption at 1652 cm^{-1} is assigned to C=O stretching or C=C stretching of conjugated or aromatic systems. Bands at 1454 cm^{-1} and 1417 cm^{-1} are associated with C–H bending and aromatic ring skeletal vibrations. The absorptions at 1329 cm^{-1} and 1275 cm^{-1} indicate C–O stretching and O–H bending vibrations, confirming the presence of phenolic or alcoholic functional groups. Strong bands observed at 1099 cm^{-1} and 1049 cm^{-1} are due to C–O stretching vibrations. Additional peaks at 890 cm^{-1}, 803 cm^{-1}, and 702 cm^{-1} correspond to out-of-plane C–H bending vibrations of substituted aromatic rings. Overall, the FTIR spectrum confirms that the compound contains hydroxyl, aliphatic, carbonyl or aromatic unsaturation, C–O functionalities, and aromatic ring structures, indicating an oxygen-rich aromatic organic compound.

Characterization And Physiochemical Evaluation Of Gel: The physical appearance of the prepared hydrogels was assessed visually under light and against white and black backgrounds. The formulations exhibited a yellowish-green color with a translucent appearance, indicating uniform gel formation. The pH of the hydrogels ranged from 5.12 to 6.45, which is within the acceptable range for topical application, minimizing the risk of skin irritation. The optimized formulation (MFG2) showed a pH of 6.45, and no significant changes in pH were observed over time, indicating good chemical stability.

Spreadability studies revealed values between 12.64 and 19.45 g·cm/s, with HPMC K-100M-based formulations showing superior spreadability compared to Carbopol 934 and guar gum gels, and all formulations performed comparably to a marketed gel. Viscosity measurements using a Brookfield viscometer indicated values ranging from 1937.49 to 3650.63 cP, exhibiting pseudoplastic behavior as viscosity decreased with increasing shear rate. Extrudability tests demonstrated that HPMC K-100M gels had excellent tube extrusion properties, whereas Carbopol 934 and guar gum gels showed satisfactory performance. These evaluations confirmed that the hydrogels possess suitable physical, mechanical, and application properties for topical delivery.

Table 2: pH, Spreadability and Viscosity of gel

Formulation	pH	Spreadability (g.cm/sec)	Viscosity (cps)
MFG1	5.32	17.64	2858.87
MFG2	6.45	15.89	3250.63
MFG3	5.99	18.15	2737.49
MFG4	6.09	14.09	2498.09
MFG5	6.25	14.25	3234.09
MFG6	5.87	13.87	2909.98

Table 3: Extrudability study of various gel formulations

Formulation	Weight of formulation	Weight of gel extruded	Extradibility amount (%)	Grade
MFG1	15.97	13.25	86.43	Good
MFG2	15.78	13.86	86.31	Good
MFG3	15.64	13.11	86.65	Good
MFG4	15.20	12.99	82.86	Good
MFG5	15.23	13.02	83.75	Good
MFG6	15.67	13.75	84.54	Good

***In-vitro* drug release study:** The in-vitro drug release profiles of formulations MFG1, MFG2, and MFG3 were evaluated over a period of 8 hours, and the cumulative percentage drug release data are presented in figure 3. All three formulations showed a time-dependent increase in drug release, indicating a controlled and sustained release pattern. At the initial stage (1–2 h), a low percentage of drug release was observed for all formulations, which may be attributed to the initial hydration and swelling of the formulation matrix. At 1 hour, the cumulative drug release was 8.12 ± 0.64% for MFG1, 9.23 ± 1.65% for MFG2, and 8.61 ± 0.89% for MFG3, indicating minimal burst release.

As the time progressed, a gradual and steady increase in drug release was observed. By 4 hours, MFG2 showed a comparatively higher release (37.19 ± 3.15%) than MFG1 (33.89 ± 2.15%) and MFG3 (35.39 ± 3.11%). This trend continued throughout the study, with MFG2 consistently exhibiting the highest cumulative drug release. At the end of 8 hours, the cumulative drug release values were found to be 84.24 ± 5.60% for MFG1, 90.24 ± 5.60% for MFG2, and 87.24 ± 5.33% for MFG3.

The higher drug release observed with MFG2 may be attributed to differences in formulation composition, such as polymer concentration or matrix structure, which could enhance drug diffusion and erosion mechanisms. Overall, all formulations demonstrated sustained drug release behavior; however, MFG2 showed the most efficient release profile, achieving nearly 90% drug release within 8 hours. Therefore, MFG2 can be considered the optimized formulation for controlled drug delivery based on its superior in-vitro release performance.

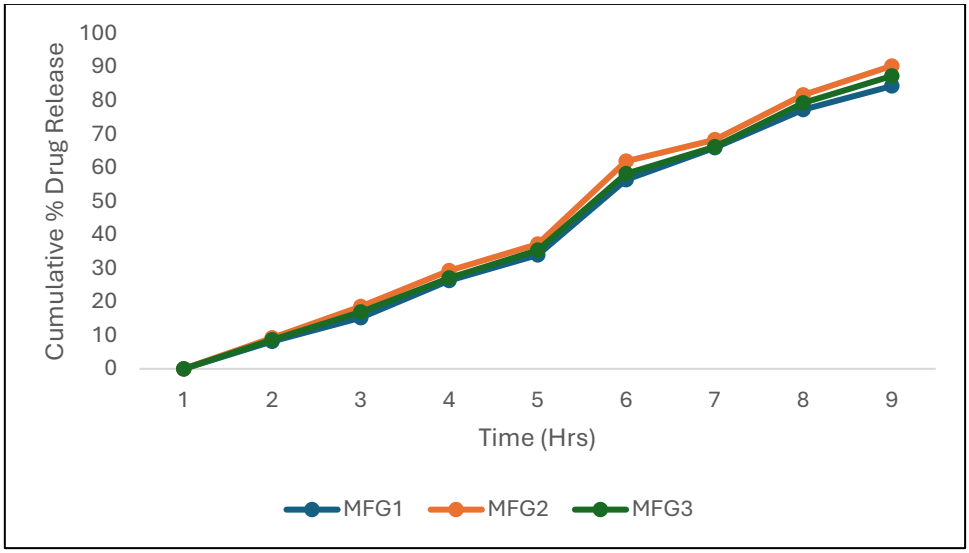

Figure 3: In-vitro drug release study of (MFG1-MFG3)

The in-vitro drug release profiles of formulations MFG4, MFG5, and MFG6 were evaluated over an 8-hour period, and the cumulative percentage drug release data are summarized in figure 4. All formulations exhibited a gradual and time-dependent increase in drug release, indicating a sustained release behavior. During the initial phase (1–2 hours), a low percentage of drug release was observed, suggesting minimal burst release. At 1 hour, the cumulative drug release was 6.12 ± 0.78% for MFG4, 7.43 ± 0.98% for MFG5, and 6.99 ± 0.98% for MFG6.

As the study progressed, a steady increase in drug release was noted for all formulations. By 4 hours, the cumulative drug release reached 33.89 ± 2.67% for MFG4, 35.16 ± 3.61% for MFG5, and 34.39 ± 1.67% for MFG6, indicating comparable release behavior

among the three formulations. However, MFG5 consistently showed a slightly higher drug release at each time point compared to MFG4 and MFG6. At the end of 8 hours, MFG4 released 78.24 ± 6.89% of the drug, whereas MFG5 and MFG6 released 86.24 ± 4.65% and 82.56 ± 3.21%, respectively.

The enhanced drug release observed in MFG5 may be attributed to optimized formulation parameters such as polymer ratio, matrix porosity, or improved drug diffusion characteristics. Overall, all three formulations demonstrated sustained drug release profiles suitable for controlled drug delivery. Among them, MFG5 showed the most favorable release pattern with higher cumulative drug release, suggesting it as a potential optimized formulation in this group.

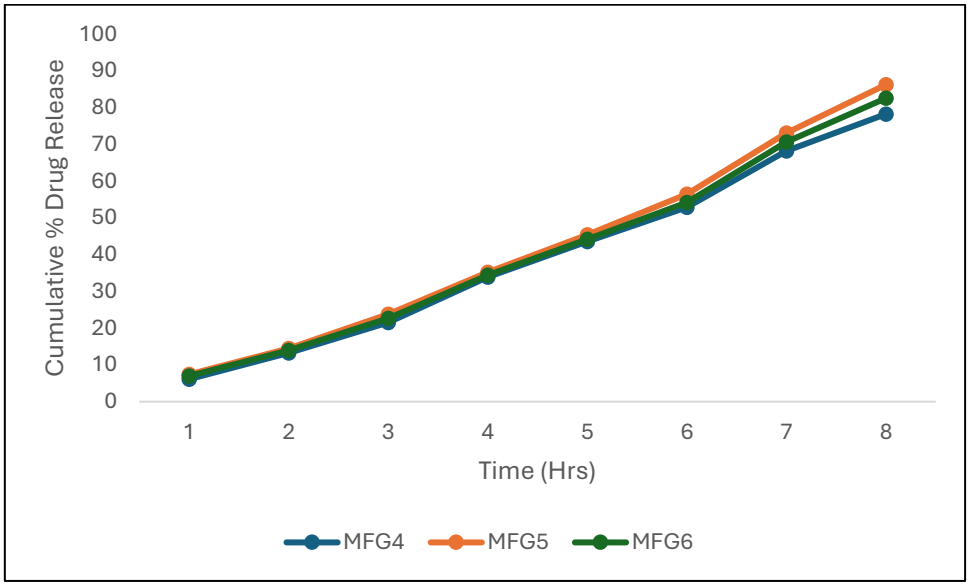

Figure 4: In-vitro drug release study of (MFG4-MFG6)

Stability Studies: The pH, viscosity, spreadability were analysed and there was a marginal difference between the formulations stored at different temperatures as shown in table 3.7. Hydrogel formulations retained good stability throughout the study.

Table 4: Stability studies

Parameters	1 month	2 months	3 months
pH	6.45	6.50	6.55
Viscosity (cps)	3250.63	3233.34	3211.56
Spreadability (gm.cm/sec)	15.89	15.11	14.34

Microbiological Evaluation of Formulated Hydrogels: The antimicrobial activity of the different gel formulations (MFG1–MFG6) was evaluated by determining their mean minimum inhibitory concentrations (MICs) against selected bacterial and fungal strains, as presented in Table 5. Lower MIC values indicate higher antimicrobial efficacy. The results demonstrate that the formulations exhibited varying degrees of antimicrobial activity depending on both the formulation composition and the test organism.

Against Staphylococcus epidermidis, formulations MFG1, MFG4, and MFG6 showed the lowest MIC value of 6.25 mg/mL, indicating strong antibacterial activity, whereas MFG5 exhibited the least activity with an MIC of 25.00 mg/mL. In the case of Staphylococcus aureus, MFG2 showed the highest efficacy with a low MIC value of 6.25 mg/mL, while most other formulations required a higher concentration (25.00 mg/mL) to inhibit growth. This suggests that MFG2 is particularly effective against S. aureus.

For the Gram-negative organism Escherichia coli, MFG2 demonstrated the strongest antibacterial activity with an MIC of 3.13 mg/mL, followed by MFG3 (6.25 mg/mL) and MFG1 (12.50 mg/mL). No inhibitory activity was observed for MFG4 against E. coli. Against Pseudomonas aeruginosa, a relatively resistant organism, only MFG2, MFG3, MFG4, and MFG6 showed inhibitory effects, with MFG6 being the most effective (MIC 12.50 mg/mL), while MFG1 and MFG5 showed no inhibition.

Table 5: Mean MICs (mg/mL) of the different gel formulation against test organisms

Gel formulations	*Staphylococcus epidermidis*	*Staphylococcus aureus*	*Escherichia coli*	*Pseudomonas aeruginosa*	*Candida albicans*
MFG1	6.25±0.02	25.00±0.05	12.50±0 05	-	12.50±0 05
MFG2	12.50±0.07	6.25±0.31	3.13±0.15	25.00±0 22	12.50±0.22
MFG3	12.50±0.10	25.00±0.22	6.25±0.21	25.00±0.10	12.50±0.08
MFG4	6 25±0.06	25.00±0.20	-	25.00±0.13	12.50 ± 0.21
MFG5	25.00 ± 0.13	25.00 ± 0.08	25.00±0.31	-	6.25 ± 0.43
MFG6	6.25±0.06	25.00 ± 0.20	25.00±0.13	12.50±0.21	-

Key: (-) no inhibition.

CONCLUSION

The present study successfully demonstrated the green synthesis of Ag/AgCl nanoparticles using morin as a biological reducing and stabilizing agent, followed by their effective incorporation into hydrogel formulations for topical application. The synthesized nanoparticles were confirmed by UV–Vis spectroscopy, and FTIR analyses, which collectively established their formation, nanoscale size, crystalline nature, stability, and the role of morin phytochemicals in reduction and stabilization. The formulated hydrogels exhibited acceptable physicochemical properties, including suitable pH, viscosity, spreadability, extrudability, and stability over time, ensuring patient compliance and formulation robustness. In-vitro drug release studies revealed sustained and controlled release behavior, with MFG2 and MFG5 emerging as optimized formulations among their respective groups. Furthermore, the microbiological evaluation demonstrated broad-spectrum antimicrobial activity against both Gram-positive and Gram-negative bacteria as well as Candida albicans, with notable efficacy shown by specific formulations depending on the microorganism. Overall, the results confirm that morin-mediated Ag/AgCl nanoparticle-loaded hydrogels are stable, effective, and promising candidates for topical antimicrobial drug delivery applications.

REFERENCES

1. World Health Organization. Global report on psoriasis. World Health Organization, 2016.
2. Hay SI, Abajobir AA, Abate KH, et al. Global, regional, and national disability-adjusted life-years (DALYs) for 333 diseases and injuries and healthy life expectancy (HALE) for 195 countries and territories, 1990-2016: A systematic analysis for the Global Burden of Disease Study 2016. Lancet 2017;390:1260–344
3. Parisi R, Iskandar IYK, Kontopantelis E, et al. National, regional, and worldwide epidemiology of psoriasis: Systematic analysis and modelling study. BMJ 2020;369:m1590.
4. Global Psoriasis Atlas. Statistics. GPA. http://global-psoriasis-atlas.apos2.swiss4ward.com/statistics/statistics#KeyMessages [Accessed 15 March 2021].
5. Dand N, Mahil SK, Capon F, et al. Psoriasis and genetics. Acta Derm Venereol 2020;100:adv00030.
6. Schön MP, Erpenbeck L. The interleukin-23/interleukin-17 axis links adaptive and innate immunity in psoriasis. Front Immunol 2018;9:1323.
7. Budu-Aggrey A, Brumpton B, Tyrrell J, et al. Evidence of a causal relationship between body mass index and psoriasis: A mendelian randomization study. PLoS Med 2019;16:e1002739.
8. Nast A, Smith C, Spuls PI, et al. EuroGuiDerm Guideline on the systemic treatment of Psoriasis vulgaris – Part 2: specific clinical and comorbid situations. J Eur Acad Dermatology Venereol 2021;35:281–317.
9. Smith CH, Yiu ZZN, Bale T, et al. British Association of Dermatologists guidelines for biologic therapy for psoriasis 2020: a rapid update. Br J Dermatol 2020;183:628–37.
10. Mahil SK, Ezejimofor MC, Exton LS, et al. Comparing the efficacy and tolerability of biologic therapies in psoriasis: an updated network meta-analysis. Br J Dermatol 2020;183:638–49.
11. Dand N, Duckworth M, Baudry D, et al. HLA-C*06:02 genotype is a predictive biomarker of biologic treatment response in psoriasis. J Allergy Clin Immunol 2019;143:2120–30.
12. Benjegerdes K, Hyde K, Kivelevitch D, Mansouri B. Pustular psoriasis: pathophysiology and current treatment perspectives. Psoriasis (Auckl) 2016;6:131–44.
13. Bachelez H, Choon S-E, Marrakchi S, et al. Inhibition of the interleukin-36 pathway for the treatment of generalized pustular psoriasis. N Engl J Med 2019;380:981–3.
14. Mahil SK, Catapano M, Di Meglio P, et al. An analysis of IL-36 signature genes and individuals with IL1RL2 knockout mutations validates IL-36 as a psoriasis therapeutic target. Sci Transl Med 2017;9:eaan2514.

15. Lee M., Cha H.J., Choi E., Han M., Kim S., Kim G.Y., Hong S., Park C., Moon S.K., Jeong S.J. Antioxidant and cytoprotective effects of morin against hydrogen peroxide-induced oxidative stress are associated with the induction of Nrf-2mediated HO-1 expression in V79-4 Chinese hamster lung fibroblasts, Int. J. Mol. Med. 39 (2017) 672–680.
16. Hyun H.B., Lee W., Go S.I., Nagappan A., Park C., Han M., Hong S., Kim G., Kim G., Cheong J. The flavonoid morin from Moraceae induces apoptosis by modulation of Bcl-2 family members and Fas receptor in HCT 116 cells, Int. J. Oncol. 6 (2015) 2670–2678.
17. Nandhakumar R., Salini K., Devaraj S.N. Morin augments anticarcinogenic and antiproliferative efficacy against 7, 12-dimethylbenz (a)-anthracene induced experimental mammary carcinogenesis, Mol. Cell. Biochem. 364 (1–2) (2012) 79–92.
18. Sivaramakrishnan V., Devaraj S.N., Morin regulates the expression of NF-κB-p65, COX-2 and matrix metalloproteinases in diethylnitrosamine induced rat hepatocellular carcinoma, Chem. Biol. Interact. 180 (3) (2009) 353–359.
19. Sivaramakrishnan V., Shilpa P.N.M., Kumar V.R.P., Devaraj S.N. Attenuation of N-nitrosodiethylamine-induced hepatocellular carcinogenesis by a novel flavonol-Morin, Chem. Biol. Interact. 171 (1) (2008) 79–88.

How to cite this article:
Khushboo et al. Ijppr.Human, 2026; Vol. 32 (4): 506-513.
Conflict of Interest Statement: All authors have nothing else to disclose.